



# Facile fabrication of novel cobalt-based carbonaceous coatings on nickel-titanium alloy fiber substrate for selective solid-phase microextraction

Junliang Du<sup>a,b</sup>, Rong Zhang<sup>a</sup>, Feifei Wang<sup>a</sup>, Hua Zhou<sup>a</sup>, Xuemei Wang<sup>a</sup>, Xinzhen Du<sup>a,\*</sup>

<sup>a</sup> College of Chemistry and Chemical Engineering, Northwest Normal University, Lanzhou 730070, China

<sup>b</sup> Department of Chemistry and Chemical Engineering, Mianyang Normal University, Mianyang 621000, China

## ARTICLE INFO

### Article history:

Received 24 June 2021

Revised 14 August 2021

Accepted 7 October 2021

Available online 13 October 2021

### Keywords:

ZIF-67

Cobalt-based carbonaceous coatings

Nickel/titanium alloy

Solid-phase microextraction

## ABSTRACT

Fabrication of selective adsorption coatings plays a crucial role in solid-phase microextraction (SPME). Herein, new strategies were developed for the *in-situ* fabrication of novel cobalt-based carbonaceous coatings on the nickel-titanium alloy (NiTi) fiber substrate using ZIF-67 as a precursor and template through the chemical reaction of ZIF-67 with glucose, dopamine (DA) and melamine, respectively. The adsorption performance of the resulting coatings was evaluated using representative aromatic compounds coupled to high-performance liquid chromatography (HPLC) with ultraviolet detection (HPLC-UV). The results clearly demonstrated that the adsorption selectivity was subject to the surface elemental composition of the fiber coatings. The cobalt and nitrogen co-doped carbonaceous coating showed better adsorption selectivity for ultraviolet filters. In contrast, the cobalt-doped carbonaceous coating exhibited higher adsorption selectivity for polycyclic aromatic hydrocarbons. The fabricated fibers present higher mechanical stability and higher adsorption capability for model analytes than the commercial polydimethylsiloxane and polyacrylate fibers. These new strategies will continue to expand the NiTi fibers as versatile fiber substrates for metal-organic frameworks (MOFs)-derived coating materials with controllable nanostructures and tunable properties.

© 2021 Published by Elsevier B.V. on behalf of Chinese Chemical Society and Institute of Materia Medica, Chinese Academy of Medical Sciences.

Sample pretreatment plays a vital role in qualitative and quantitative analysis of various analytes in complex matrices [1,2]. Solid-phase microextraction (SPME) is an ideal tool for sample pretreatment because of its low solvent consumption, simple operation and easy automation with analytical instruments [3,4]. This technique integrates sampling with sample preparation, leading to the combined extraction and enrichment of target analytes [5]. In the case of fiber configuration, SPME greatly depends on the nature of the sorbent coated on the fiber substrate [6]. Therefore, the development of novel fiber coatings is the key factor for SPME. Several commercial coatings, such as polyacrylate (PA) and polydimethylsiloxane (PDMS) have been widely used in SPME. Nevertheless, the applications of commercially available fused-silica fibers with polymeric coatings are subject to their fragility, relatively low thermal stability, inferior solvent resistance, poor extraction selectivity, short service life and high cost [7]. A variety of materials have been developed as fiber coatings including carbon materials, metal ox-

ides, polymers, layered double hydroxides, covalent organic frameworks, metal-organic frameworks (MOFs) and their composites [8–13].

Among aforementioned coatings, MOFs-derived carbonaceous materials have been introduced into SPME as a group of emerging adsorbents due to their intrinsic advantages such as high porosity, permanent nanoscale cavities and open channels [14]. In practical SPME applications, these MOFs-derived carbonaceous coating materials were initially immobilized onto metallic fiber substrates by using neutral silicone sealant or sol-gel solution as the binders [15,16]. In these cases, the binders could cover the active sites and lessen the adsorption ability to some extent. As compared with conventional powdery MOFs-derived carbonaceous coatings, the self-supported coatings grown on the fiber substrates are more desirable as they could avoid the addition of organic binders and ensure the seamless contact between coating materials and fiber substrates, leading to the improvement of the surface adsorption performance by adjusting the morphology and microstructure [17,18]. This new strategy for the *in-situ* conversion of MOFs into carbonaceous materials on the metallic fiber substrates is further needed to be exploited in practical SPME applications.

\* Corresponding author.

E-mail address: [duxz@nwnu.edu.cn](mailto:duxz@nwnu.edu.cn) (X. Du).

Recently, more and more studies have demonstrated that MOFs, particularly zeolitic imidazolate frameworks (ZIFs), are one type of ideal sacrificial precursors for synthesizing metal/metallic compounds/N-doped carbonaceous materials *via* high-temperature pyrolysis strategy [1,19,20]. Furthermore, they are also regarded as versatile templates for the derivation of carbonaceous materials through chemical reaction of ZIFs with organic carbon precursors [21–23]. In this work, the Co coating was electrochemically deposited on the nickel-titanium alloy (NiTi) fiber substrate as Co ion sources for subsequent electrochemical *in-situ* growth of ZIF-67 on the NiTi fiber substrate. By choosing ZIF-67 as a precursor and template, multiple ZIF-67-derived carbonaceous coatings were *in-situ* fabricated on the superelastic NiTi fiber substrate through the reaction of ZIF-67 with glucose, dopamine (DA) and melamine, respectively. The adsorption performance of the resulting coatings with different elemental compositions was evaluated using typical chlorophenols (CPs), phthalic acid esters (PAEs), ultraviolet filters (UVFs) and polycyclic aromatic hydrocarbons (PAHs) as model analytes coupled to HPLC-UV.

The detailed fabrication processes were presented in Supporting information. The bare NiTi wire was pretreated prior to use. As shown in Fig. S1 (Supporting information), the bare NiTi wire demonstrated relatively smooth surface with some microcracks at high magnification (Figs. S1a and b). A native surface passivation layer was present according to the contents of Ni, Ti and O elements (Fig. S2a in Supporting information). After acid treatment, the sparse particle coating appeared (Figs. S1c and d) and only Ni and Ti elements were detected at the surface of the pretreated NiTi wire (Fig. S2b in Supporting information), indicating that the surface passivation layer was removed. As shown in Figs. S1e, S1f and S2c (Supporting information), Co nanoflakes were electrochemically grown on the pretreated NiTi wire, resulting in the fabrication of the NiTi@Co fiber. Subsequently the Co coating was electrochemically *in-situ* anodized. In this case,  $\text{Co}^{2+}$  was generated *via* the anodic dissolution of the Co coating, and then coordinates with 2-methylimidazole (2-MIM) in the electrolyte. The magnified SEM image (Fig. S1h) clearly demonstrated the tetrahedral cone-shaped coating with distinct facets, straight edges, and smooth exterior surfaces. Energy dispersive X-ray spectroscopy (EDX) analysis revealed the coexistence of C, N and Co elements with a mass fraction of 47.99%, 20.98% and 31.03%, respectively (Fig. S2d in Supporting information). This result indicated that ZIF-67 was successfully formed on the NiTi@Co fiber, in good agreement with its stoichiometric ratio [24]. As compared with that needed time for the growth of ZIF-67 in ethanolic solution [25], the time for the electrochemical *in-situ* growth of ZIF-67 on the NiTi@Co fiber is greatly reduced from 32 h to about 11 min, indicating that the electrochemical *in-situ* transformation of Co into ZIF-67 possesses advantage of much less time consumption.

Polydopamine (PDA) has been identified as an appealing coating on ZIF surface due to its facile polymerization, sufficient N content and abundant active groups [21]. In the presence of DA, the catechol groups of DA coordinate with  $\text{Co}^{2+}$  of ZIF-67, and the released 2-MIM with Lewis base groups triggers the formation of PDA, dispensing with the need for the introduction of alkali. Fig. 1 presented the SEM images of the fabricated coatings after ZIF-67-triggered polymerization of DA and after pyrolysis. When coated with PDA, the surface of the fiber coating became coarse accompanied by the appearance of distinct nanoparticles with high specific surface area. As can be seen from corresponding EDX signals and data in Fig. S3a (Supporting information), the O element appears, indicating that PDA was successfully formed on the surface of ZIF-67. After pyrolysis in  $\text{N}_2$  atmosphere (Fig. 1b), the resulting coating showed similar morphology to that of the ZIF-67@PDA coating. EDX analysis in Fig. S3b (Supporting information) also revealed that the Co and N co-doped (Co-NC) coating was derived

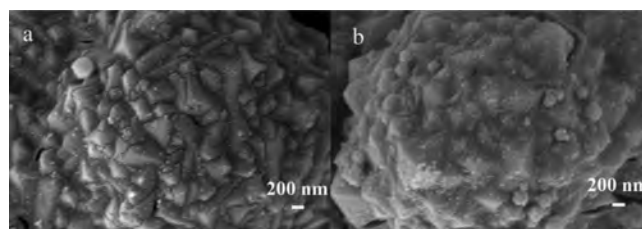


Fig. 1. SEM images of the Co@ZIF-67@PDA (a) and the Co-NC (b) coatings.

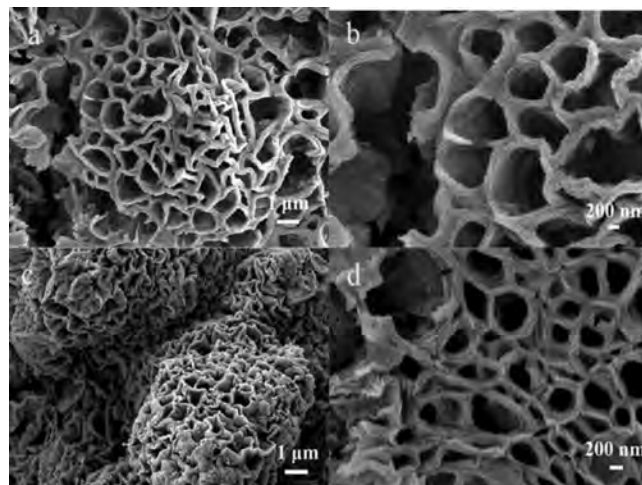
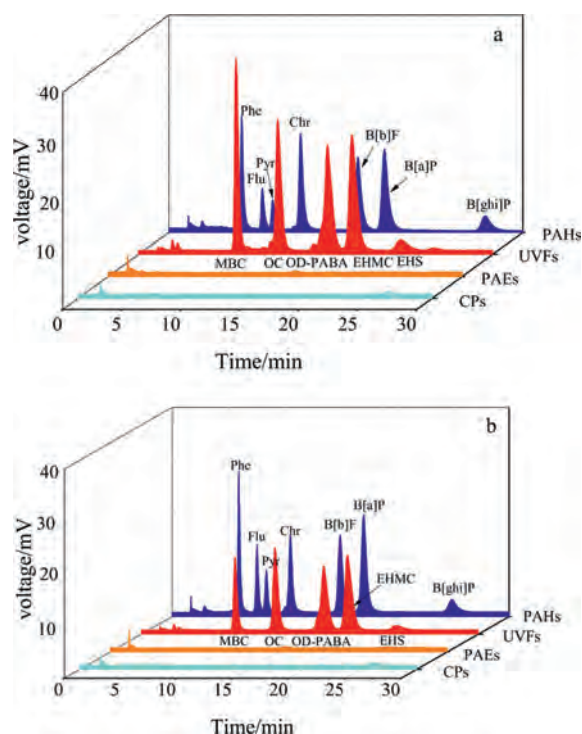


Fig. 2. SEM images of the fiber coatings at low ( $\times 20,000$ ) and high magnification ( $\times 50,000$ ) after the reaction of ZIF-67 coating with glucose (a, b) and after pyrolysis (c, d).

from direct pyrolysis of the ZIF-67@PDA coating. As a result, the resulting fiber was denoted as the NiTi@Co-NC fiber.

Glucose also had a significant effect on the morphology of ZIF-67. As shown in Fig. 2, the ZIF-67-derived coating exhibited a porous structure after the hydrothermal reaction of ZIF-67 with glucose (Figs. 2a and b). This result can be attributed to the etching and polymerization of glucose [22]. In the initial stage of the hydrothermal reaction, the oxidation of glucose generates acids which can etch the ZIF-67 crystal. Subsequently the decomposed ZIF-67 reacts *in-situ* with the glucose-derived polymers, forming a composite layer. Simultaneously the hydrolysis of  $\text{Co}^{2+}$  from the decomposed ZIF-67 would further decrease the solution pH and accelerate the etching of ZIF-67 [26]. As can be seen from Fig. S4a (Supporting information), the disappearance of N element suggested that ZIF-67 was completely decomposed. Thereafter, the hierarchical porous coating was derived from direct pyrolysis in  $\text{N}_2$  atmosphere and the resulting coating inherited the porous morphology of the former (Figs. 2c and d). Corresponding EDX analysis confirmed that the resulting coating was composed of C, O and Co elements with a mass fraction of 10.03%, 15.32% and 74.65%, respectively (Fig. S4b in Supporting information). In this case, the porous Co-doped carbonaceous (Co-C) coating was achieved on the NiTi fiber substrate using ZIF-67 as a precursor and template through the chemical reaction of ZIF-67 with glucose. The resulting fiber was denoted as the NiTi@Co-C fiber.

The influence of melamine on the morphology of the ZIF-67 coating was further examined. As shown in Fig. S5a (Supporting information), the similar surface morphology was obtained by *in-situ* reaction of ZIF-67 with melamine compared to that of the ZIF-67 coating (Fig. S1h). According to EDX data in Fig. S5b (Supporting information), the N content greatly increased, and the C content remarkably decreased in the resulting coating, while the Co con-



**Fig. 3.** Typical chromatograms of SPME-HPLC with the NiTi@Co-NC fiber (a) and the NiTi@Co-C fiber (b) for PAHs, UVFs, CPs and PAEs.

tent slightly changes compared with that of ZIF-67 (Fig. S2d). This result indicates that another novel Co and N co-doped carbonaceous coating was formed on the NiTi fiber substrate. However, in practical SPME application, the resulting coating was easily peeled off. The fabricated fiber was not suitable for SPME. Therefore, this fiber was not discussed further in subsequent study.

The adsorption performance of the fabricated carbonaceous coatings was compared using CPs, PAEs, UVFs and PAHs as model analytes. As can be seen in Fig. 3, the NiTi@Co-NC fiber exhibited higher adsorption capability for UVFs than for PAHs (Fig. 3a). On the contrary, the NiTi@Co-C fiber showed higher adsorption capability for PAHs than for UVFs (Fig. 3b). However, these carbonaceous coatings exhibited almost negligible adsorption capability for hydrophilic CPs and PAEs, indicating that the NiTi@Co-NC fiber could be used as a potential fiber to adsorb UVFs and the NiTi@Co-C fiber could be used for selective adsorption of PAHs.

The adsorption performance of the NiTi@Co-C and the NiTi@Co-NC fibers was further compared with the commercial PDMS and PA fibers for the extraction of PAHs. According to Fig. S6 (Supporting information), the NiTi@Co-C fiber exhibited better adsorption capability for the studied PAHs compared to the NiTi@Co-NC fiber. This result indicated that the N-deficient Co-C coating is more hydrophobic with better adsorption selectivity for PAHs. The hydrophobic interaction [25], electron donor-acceptor interaction [27] and the  $\pi$ - $\pi$  interaction between PAHs and the Co-C coating [28] may be responsible for its high adsorption capacity of the NiTi@Co-C fiber for PAHs. The adsorption properties of carbonaceous coatings are enhanced due to N-doping into the carbonaceous structure [29]. This may be caused by the nitrogen-containing groups that increase the polarity of the carbonaceous coating surface [30]. Therefore, N-doping can modify the elemental composition of the carbonaceous coatings and tailor the hydrophilicity and hydrophobicity of the carbonaceous coatings at the same time. As compared with commercial PDMS and PA fibers, the NiTi@Co-C fiber and the NiTi@Co-NC fiber also exhibited higher

adsorption capability than the PDMS fiber (except for Phe) and the PA fiber for the studied PAHs. In particular, the recoveries from 92.3% to 94.1% and 91.7% to 93.5% were achieved for spiking water at the level of 50  $\mu\text{g/L}$  after 120 cycles of adsorption and desorption for the NiTi@Co-C and NiTi@Co-NC fibers, respectively. As a result, the fabricated fibers also presents high recycling stability in practical SPME application.

In this work, new strategies were developed for the fabrication of multiple Co-based carbonaceous coatings through the reaction of ZIF-67 with glucose, DA and melamine under different conditions. Different procedures would result in different morphologies and elemental compositions of the carbonaceous coatings, and greatly affected their adsorption capability and potential adsorption selectivity. It was found that the NiTi@Co-NC fiber showed better adsorption selectivity for less hydrophilic UVFs, whereas the NiTi@Co-C fiber exhibited higher adsorption selectivity for hydrophobic PAHs. In particular, the NiTi@Co-C and the NiTi@Co-NC fibers present higher mechanical stability and better adsorption performance for PAHs compared to the commercial PDMS and PA fibers. Moreover, the template-directed fabrication of the carbonaceous coatings could be precisely controlled. These new strategies will continue to expand the NiTi wires as versatile fiber substrates for MOFs-derived coating materials with controllable nanostructures and tunable properties.

#### Declaration of competing interest

The authors declare that they have no known competing financial interests or personal relationships that could have appeared to influence the work reported in this paper.

#### Acknowledgment

This project was financially supported by the National Natural Science Foundation of China (Nos. 21765020 and 21265019).

#### Supplementary materials

Supplementary material associated with this article can be found, in the online version, at doi:10.1016/j.ccl.2021.10.007.

#### References

- [1] X.R. Hu, C.H. Wang, R. Luo, et al., *Nanoscale* 11 (2019) 2805–2811.
- [2] H.M. Liu, H. Yu, P. Jin, et al., *Chem. Eng. J.* 379 (2020) 122405.
- [3] M.Y. Ma, L.Q. Yu, S.W. Wang, Y. Meng, Y.K. Lv, *ACS Appl. Bio Mater.* 4 (2021) 3608–3613.
- [4] N. Looby, T. Vasiljevic, N. Reyes-Garcés, et al., *Talanta* 225 (2021) 121945.
- [5] D.A. Rickert, V. Singh, M. Thirukumaran, et al., *Environ. Sci. Technol.* 54 (2020) 15789–15799.
- [6] H.D. Li, B.X. Hou, L. Wang, et al., *J. Sep. Sci.* 44 (2021) 1521–1528.
- [7] Q.Q. Li, W.M. Zhang, Y.H. Guo, et al., *J. Chromatogr. A* 1646 (2021) 462031.
- [8] M. Sun, S. Han, H.M. Loussala, et al., *Microchem. J.* 166 (2021) 106263.
- [9] J.B. Qu, Y.Y. Lin, Q. Li, et al., *J. Chromatogr. A* 1639 (2021) 461928.
- [10] P. Qin, W.L. Zhu, L.Z. Han, et al., *Microchim. Acta* 187 (2020) 367.
- [11] H. Qi, Z. Li, H.J. Zheng, L. Fu, Q. Jia, *Chin. Chem. Lett.* 30 (2019) 2181–2185.
- [12] Y. Wang, Q. Ye, M.H. Yu, X.J. Zhang, C.H. Deng, *Chin. Chem. Lett.* 31 (2020) 1843–1846.
- [13] X.W. Zhang, Y.X. Yang, P.G. Qin, et al., *Chin. Chem. Lett.* 33 (2022) 903–906.
- [14] H.X. Duo, X.F. Lu, S. Wang, X.J. Liang, Y. Guo, *TrAC-Trends Anal. Chem.* 133 (2020) 116093.
- [15] X. Zhang, X.H. Zang, J.T. Wang, et al., *Microchim. Acta* 182 (2015) 2353–2359.
- [16] Q.K. Hu, S.Q. Liu, X. Chen, et al., *Anal. Chim. Acta* 1047 (2019) 1–8.
- [17] F.X. Wei, Y.H. He, X.L. Qu, et al., *Anal. Chim. Acta* 1078 (2019) 70–77.
- [18] S.T. Sun, L.J. Huang, H.Y. Xiao, Q. Shuai, S.H. Hu, *Talanta* 202 (2019) 145–151.
- [19] S. Zhang, Q. Yang, Z. Li, et al., *Analyst* 141 (2016) 1127–1135.
- [20] X. Hu, C. Wang, J. Li, et al., *ACS Appl. Mater. Interfaces* 10 (2018) 15051–15057.
- [21] T. Wang, Y. He, Y.J. Liu, et al., *Nano Energy* 79 (2021) 105487.
- [22] P. Zhang, F. Sun, Z.H. Xiang, et al., *Energy Environ. Sci.* 7 (2014) 442–450.
- [23] L.J. Yang, H. Li, Y. Yu, Y. Wu, L. Zhang, *Appl. Catal. B* 271 (2020) 118939.
- [24] J.S. Meng, C.J. Niu, L.H. Xu, et al., *J. Am. Chem. Soc.* 139 (2017) 8212–8221.

- [25] J.L. Du, R. Zhang, F.F. Wang, X.M. Wang, X.Z. Du, *J. Chromatogr. A* 1618 (2020) 460855.
- [26] J. Wang, X.L. Luo, C. Young, et al., *Chem. Mater.* 30 (2018) 4401–4408.
- [27] J. Xu, P. Wu, E.C. Ye, B.F. Yuan, Y.Q. Feng, *TrAC-Trends Anal. Chem.* 80 (2016) 41–56.
- [28] B.N. Bhadra, J.K. Lee, C.W. Cho, S.H. Jhung, *Chem. Eng. J.* 343 (2018) 225–234.
- [29] Q. Li, H.Y. Pan, D. Higgins, et al., *Small* 11 (2015) 1443–1452.
- [30] E. Lorenc-Grabowska, G. Gryglewicz, J. Machnikowski, *Appl. Surf. Sci.* 256 (2010) 4480–4487.